STRUCTURAL RESPONSE OF THE EADF TARGET BEAM WINDOW TO BEAM INTERRUPTIONS: TRANSIENT THERMO-MECHANICAL COMPUTATIONS

G. Fotia, C. Aragonese, V. Bellucci, S. Buono, L. Maciocco,
V. Moreau, G. Siddi, L. Sorrentino
CRS4, Center for Advanced Studies, Research and Development in Sardinia
Cagliari, Italy

Abstract

The operability of a high power proton beam target in an Accelerator Driven System (ADS) is strictly connected to the structural integrity of the beam window, which is undoubtedly the most delicate component in such devices, being exposed to the combined effects of high intensity proton and neutron irradiation, liquid metal corrosion and high thermal stresses induced by the interaction with the beam. It has also recently been highlighted that beam trips may frequently occur in current high power accelerators [1]. Clearly, the definition of the requirements of future accelerators depends on the behaviour of the window under such conditions. For this purpose a numerical study of typical transients has been carried out on the 600 MeV proton beam target that drives the 80 MW Demonstration Facility of the Energy Amplifier proposed by C. Rubbia, [2] presently under development in Italy by Ansaldo, CRS4, ENEA and INFN [3].

EADF beam target description

The Energy Amplifier Demonstration Facility (EADF) is a nuclear system in which an external source of neutrons drives a subcritical core. Neutrons come from the interaction of a high power proton beam with a high Z material contained in the accelerator target. Such interaction, called spallation, has the undesirable effects of producing a large quantity of heat (typically some MW concentrated in a small volume) and inducing an intense radiation damage in the structural materials. Liquid metals are currently considered the best choice in terms of target materials since they satisfy the important criteria of being the spallation medium and the cooling fluid at the same time and since their structural and thermal properties are not degraded by the radiation damage induced by protons interactions. We selected the Lead-Bismuth Eutectic (LBE) as a spallation target material since it joins good neutronic properties to a relatively low melting point (125 ^{o}C), that simplify the operability of the target.

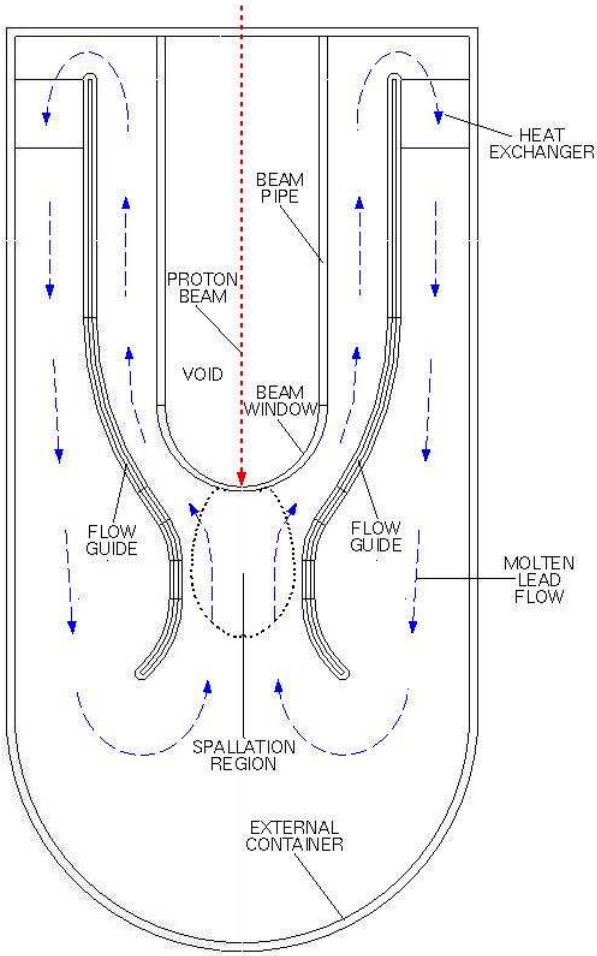

Figure 1 - Scheme of the EADF target

The EADF target [4] scheme is illustrated in figure 1. It consists of a 20 cm external diameter vertical beam pipe enclosed in a coaxial container. The beam pipe is closed at the bottom by a beam window. The beam window has a hemispherical external surface and an ellipsoidal internal surface so

Invited paper to the Second OECD/NEA workshop on utilisation and reliability of high power accelerators, Aix en Provence, France, 22-24 November 1999

that the thickness varies from a minimum of 1.5 mm in the beam axis to a maximum of 3 mm in the junction with the beam pipe. The tapering reduces the heat deposit in the centre of the window, where the proton flux is higher. The beam window material is a martensitic 9Cr 1Mo V Nb steel which has been selected by ENEA [5] because of its relatively high thermal conductivity, low thermal expansion coefficient, high resistance to neutron induced swelling and high temperature stresses and good corrosion compatibility with LBE. The container is a vertical cylinder of 27 cm radius and 7 m height with a hemispherical bottom.

The region between the beam pipe and the container is filled with LBE and vacuum is made inside the beam pipe. The heat produced in the window and in the coolant is removed by a natural convection flow. The flow guide separates the hot rising liquid from the cool liquid flowing out of the heat exchanger positioned on the top. In the spallation region the flow guide assumes a funnel shape which accelerates the flow and enhances the cooling of the window. The proton beam is injected through the top of the beam pipe. The proton energy is 600 MeV and the beam size is assumed to be a circular spot of 7.5 cm radius. Beam defocusing prevents localised high power densities in the target structures. The beam current distribution follows a parabolic profile. The maximum nominal beam current is 6 mA corresponding to a beam power of 3.6 MW.

Structural integrity assessment of the beam window

High power proton accelerators are being utilised in many ADS projects. In these applications the accelerator reliability, especially for beam trips and power fluctuations, is extremely important and can be determinant for the possible utilisation of these machines in the future [1]. Accelerators beam stability failures lead to beam interruptions inducing large and rapid thermal transients in all components that are directly exposed to the beam and particularly in the window. As a typical example, the maximum temperature of the EADF window after a beam interruption decreases from 490°C to about 210°C in a time of about 6 s. The evaluation of the structural integrity of the beam window during its operating life is therefore an important step toward the assessment of the design of the EADF target. In particular, thermal fatigue and possibly creep-fatigue failure life should be properly assessed, either by thermal transient strength tests or by computational models.

Transient thermal-mechanical modelling of the beam window response

In the following sections, we will illustrate a computational model of the beam window under thermal transients. We will first present the assumptions that have been adopted and then the effective computational strategy for solving the time dependent heat transfer and stress analysis coupled problem of interest. Finally, the numerical model of the EADF target is presented with some detail.

Modelling assumptions

The non-stationary coupled problem of the interacting coolant flow and the beam window structure is governed by the (time dependent) Navier-Stokes equations and by the energy conservation equations. In the solid, the displacements fields are derived by imposing equilibrium and compatibility conditions.

In the model the following assumptions have been considered:

1 - Structural displacements do not influence the thermal-hydraulic field.

2 - Displacement characteristic times are much smaller than temperature variation times, so that the structural problem can be considered quasi-static.

The displacement field of the structure can be computed once the thermal field in the solid is known from the solution of the thermal-hydraulic problem. The following strategy is therefore applied:

1. Calculate the heat source distribution.

2. Calculate the transient for the velocity field in the fluid and for the thermal fields in both the fluid and the solid.

3. Given the computed temperature maps in the solid at discrete points along the time sequence of interest, solve for the displacement and stress field in the solid.

In the following, a linear elastic small-deformation model is assumed for the structure. Temperature dependent material properties have been considered.

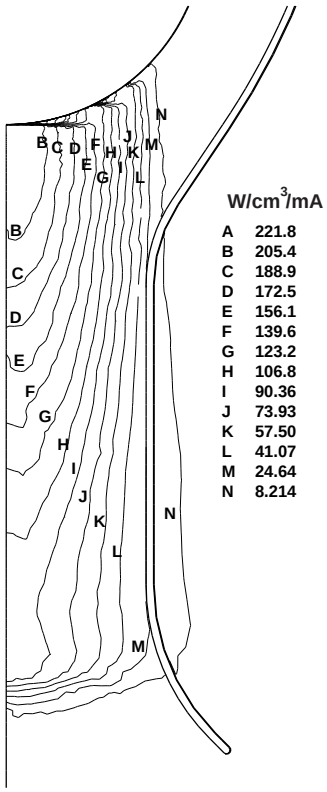

Figure 2 - Map of the power generated in the EADF target by the 600 MeV proton beam

Numerical model of the EADF target

Neutronics

The FLUKA Monte-Carlo code [6] is employed to determine the heat source distribution to be used as input for the CFD computations. According to the results of the FLUKA simulations, the proton beam releases in the window about 22 kW (i.e. 0.6% of the total beam power). The heat production in the coolant and in the flow guide accounts for about the 72% and the 1% of the total, the remaining part of the beam energy being contained in the particles escaping the system or in the binding energy of the target nucleus. Figure 2 shows the distribution of the heat source in the target.

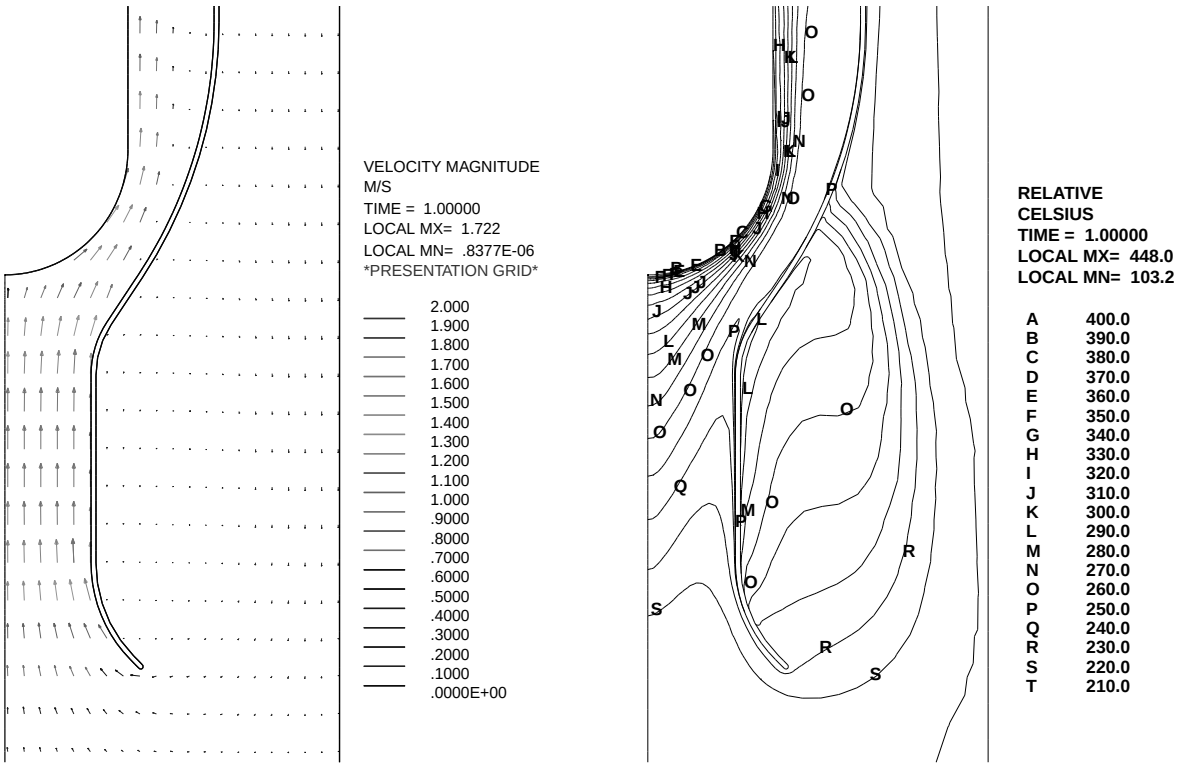

Figure 3 – Velocity and temperature fields in the funnel region.

Fluid dynamic and heat transfer modelling

The turbulent natural convection flow of the coolant and the thermal field in the beam window are simulated using STAR-CD v3050A. A mixed structured/unstructured mesh of about 24,000 cells is employed, with a very accurate discretisation in the funnel zone, especially in the vicinity of the window stagnation point, where the most severe gradients of the fields' variables are expected. The numerical model is based on an axisymmetric finite-volume formulation and employs a third order

QUICK scheme for the spatial discretisation of the convective terms. The Chen k-ε model with a two-layer algorithm in the near wall region accounts for turbulence effects. A PISO implicit algorithm is used for the time accurate simulation of the transient processes. Figure 3 shows the steady state computed velocity and temperature fields at the maximum beam current (6 mA).

Beam window structural model

A detailed MSC/NASTRAN v70.5 linear elastic finite element model of the window/pipe system has been used to predict for each discrete time the stress field induced by the (computed) thermal strain distribution and by the coolant hydrostatic pressure applied onto the external surface of the window. The model, due to geometrical and applied load axial symmetry, consists of a 5 degree portion of the complete beam pipe/window system. The 9Cr 1Mo V Nb martensitic steel has been used as the reference material for both the beam window and the pipe. Its main properties are summarised in Table 1.

		20^{0}C	**200^{0}C**	**300^{0}C**	**400^{0}C**	**500^{0}C**	**600^{0}C**
Young modulus	[MPa]	218	207	199	190	181	168
Thermal expansion coefficient	[10^{-6}/K]	10.4	11.3	11.7	12.0	12.3	12.6
Poisson ratio		0.29	0.29	0.29	0.29	0.29	0.29
Density	[Kg/m^3]	7730	7680	7650	7610	7580	7540
Thermal conductivity	[W/mK]	26	28	28	29	30	30
Yield Strength	[MPa]	539	500	495	480	400	310

Table 1 - Mechanical properties of the 9Cr 1Mo V Nb martensitic steel.

Computational results

Selection of the test cases

We have chosen the test cases with the objective of analysing the most critical situations from the point of view of window stresses. Simulating a beam interruption, we observed that the maximum stress occurs after 0.3 s [7]. We decided to investigate the effect of a beam interruption in the immediate vicinity of this typical time, namely 0.1, 0.3 and 1 s.

Another effect that can be observed during the shutdown transient is the decreasing of the coolant mass flow rate, due to the reduced natural circulation pumping force. This phenomenon, which becomes significant after several seconds, reduces the window heat removal in case of beam restart after a long interruption. In order to verify the magnitude of this problem two more transients were considered:

a) a restart after 21 seconds of beam interruption, where the velocity near the window is about 60% of its nominal value;

b) a normal start-up, where the nominal velocity in the system is imposed by an external pumping device (for example the insertion of argon bubbles in the riser), to avoid thermal transients beyond nominal conditions.

The computational effort for a typical run is about 30 CPU hours per second of simulation on a HP 780J2 workstation. A summary of the computations that have been carried out in the present study is presented in Table 2.

Test Case	***Maximum temperature***	***Maximum Tresca stress***		***Δ maximum Tresca stress***	
	[°C]	*[MPa]*	*α [degree]*	*[MPa]*	*α [degree]*
0.1 s beam interruption	490	143	26 °	73	40 °
0.3 s beam interruption	492	194	30 °	140	41°
1 s beam interruption	494	194	30 °	140	41°
21 s beam interruption	601	217	48 °	138	41°
Normal Start-up	498	167	48 °	145	45 °

Table 2 - Test cases and results summary. The location of stresses in the window is expressed with the angle α with the beam axis.

Discussion of the results

The first objective in the target transient behaviour analysis is to identify the timescale where the more interesting phenomena occur. Figure 4a shows the inertia of the whole target system during a beam shutdown followed by a restart after 21 s. Velocities decrease to about 60% of their nominal value since the pumping effect due to natural convection decreases with the temperature difference between the riser and the downcomer.

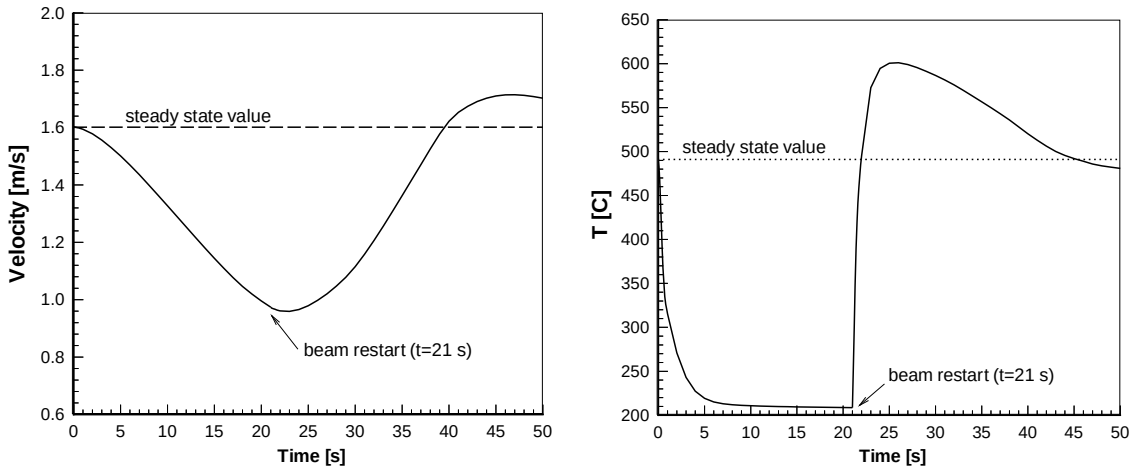

(a) (b)

Figure 4 - Maximum mean velocity in the funnel and temperature in the window during the 21 s beam interruption.

Invited paper to the Second OECD/NEA workshop on utilisation and reliability of high power accelerators, Aix en Provence, France, 22-24 November 1999

At the beam restart the initial lower mass flow rate causes higher temperatures in the hot riser column. The result is that velocities increase beyond their nominal value after about 40 s and start a damped oscillation around the steady state value until they reach a new equilibrium. This mechanism influences the cooling of the window and increases its temperature beyond its nominal value as it can be seen in figure 4b.

A possible mechanism to avoid the rise of the window temperature beyond its nominal value is to introduce at start-up an external pumping device (for example the insertion of argon bubbles in the riser) to enhance natural circulation. The comparison between a normal start-up procedure (where velocities are already at steady state values) and a beam restart after 21 s is shown in figure 5. A normal start-up procedure avoids the oscillation of window temperatures around the steady state value and reduces the peak in the hoop stress transient of the beam window, as it can be seen in figure 5b.

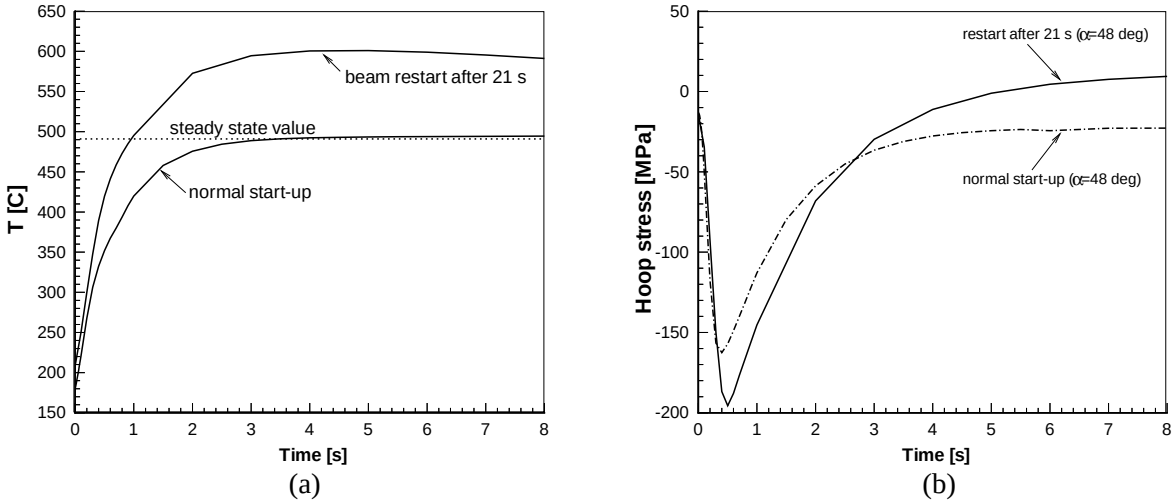

Figuew 5 – Comparison of maximum temperatures and hoop stresses in the window between a normal start-up and a beam restart after a trip of 21 s.

Figure 6a shows the maximum temperatures generated in the window during the short transients. Because of the small thermal capacity of the beam window, temperature transients are very short. As far as stresses are concerned, the radial component of the stress tensor is one order of magnitude smaller than the other two, while the values of the meridional and hoop components are quite similar, so only the latter is reported (Figure 6b). In this figure the hoop stress variation is reported in the point where this component reaches its maximum, which is located on the external surface of the window. A beam interruption has the effect of increasing the state of the stress and deformation of the window with respect to its nominal value, depending on the interruption time. For a beam stop the maximum value of the stresses is reached after 0.3 s [7]. For shorter interruptions this value is never reached whereas for interruptions longer than 0.3 s this maximum value is not overcome, but the behaviour after the peak is significantly different. In the case of the 1 s interruption there is a local sign inversion of the hoop stress showing that traction stresses are followed by compression. After beam restarts, the window quickly comes back to steady state stress conditions.

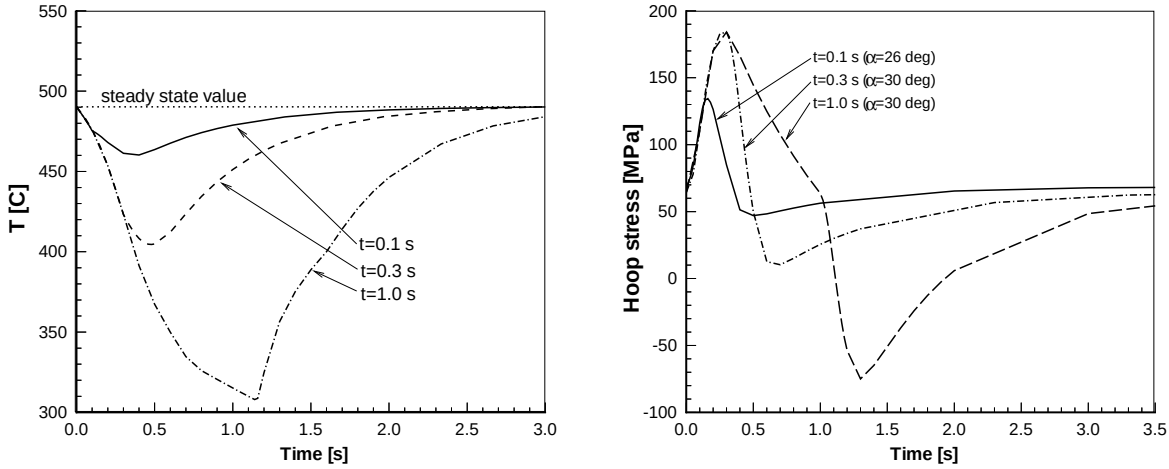

(a) (b)

Figure 6 - Maximum temperatures and hoop stresses in the window during beam interruptions (positive values of the stresses indicate tensile stresses).

A summary of the results is also presented in Table 2. One can observe that the maximum Tresca stresses occur at different locations in the beam window. The angle α is measured from the beam axis. At steady state conditions $\alpha \sim 0$. The local maximum stress differences (Δ maximum Tresca), that are representative of the thermal fatigue damage, are reasonably low and occur at different locations with respect to the maximum values. According to [8] we could in fact estimate the allowed number of cycles for non-irradiated material in excess of 10^5, but this number can dramatically decrease in real operating conditions. We can finally observe that beam interruptions of the order of tens of seconds should probably be avoided in favour of a normal start-up operation, although this kind of considerations can be more precise only after a detailed experimental campaign.

Concluding remarks

A numerical study has been carried out to evaluate the thermo-mechanical response of the EADF beam window to beam interruptions. An effective computational procedure for the resolution of the time dependent thermo-mechanical coupled problem of the interacting coolant flow and the beam window structure that allows a one-way coupling of the field variables has been adopted. Results have been presented for a significant number of cases. In particular, time histories of the response quantities (temperature and stresses in the window) are presented and discussed.

On the basis of our numerical studies the thermal transient stresses in the window are below the allowable strength limit of the material. Furthermore, the time varying stresses are below the fatigue limit of the non-irradiated steel but severe uncertainties arise from the unknown influence of neutron and proton damage, corrosion embrittlement and high concentrations of helium, hydrogen and other spallation impurities. Reliable lifetime estimates, that must include the above effects, are thus not possible at present. Material fatigue tests under proton irradiation are required for the design of future high power proton targets.

Invited paper to the Second OECD/NEA workshop on utilisation and reliability of high power accelerators, Aix en Provence, France, 22-24 November 1999

References

[1] Proceedings of the *First OECD/NEA workshop on utilisation and reliability of high power accelerators*, Mito, Japan, 13-15 October 1998.

[2] C. Rubbia et al., *Conceptual Design of a Fast Neutron Operated High Power Energy Amplifier*, CERN Report, CERN/AT/95-44 (ET), Geneva, September 29, 1995.

[3] Ansaldo, CRS4, ENEA, INFN, *Energy Amplifier Demonstration Facility Reference Configuration. Summary Report*, Ansaldo Report EA B0.00 1 200, Genova, January 1999.

[4] L. Maciocco, V. Bellucci, S. Buono, G. Fotia, V. Moreau, M. Mulas, G. Siddi, L. Sorrentino, *Design and Optimisation of a Liquid Metal Spallation Target for the Energy Amplifier Prototype*, 2nd International Topical Meeting on Nuclear Applications of Accelerator Technology, Gatlinburg, TN, USA, September 20-23, 1998.

[5] G. Beneamati and P. Buttol, *Materials selection for reactor components of an ADS demonstrator*, ENEA/HS-A-R-003.

[6] A. Fassò et al., *FLUKA92*, Workshop on Simulating Accelerator Radiation Environments, Santa Fe, USA, January 11-15, 1993. See also: A. Ferrari and P.R. Sala, *Improvements to the Electromagnetic part of the FLUKA code*, MC93 Int. Conf. on Monte-Carlo Simulation in High-Energy and Nuclear Physics, Tallahassee, February 22-26, 1993.

[7] V. Bellucci, S. Buono, G. Fotia, L. Maciocco, V. Moreau, M. Mulas, G. Siddi, L. Sorrentino, *Thermo-mechanical stresses on the beam window of the EADF*. Proceedings of the *First OECD/NEA workshop on utilisation and reliability of high power accelerators*, Mito, Japan, 13-15 October 1998.

[8] I. Alvarez-Armas, A.F. Armas and C. Petersen, *Thermal fatigue of a 12%chromium martensitic stainless steel*, Fatigue & Fracture of Eng. Materials & Structures, Vol.17, No.6, 1994

Invited paper to the Second OECD/NEA workshop on utilisation and reliability of high power accelerators, Aix en Provence, France, 22-24 November 1999